Conf-9210213--3

LBL-32926
UC-400

Lawrence Berkeley Laboratory
UNIVERSITY OF CALIFORNIA

ENERGY & ENVIRONMENT DIVISION

Presented at the Western States/The Combustion Institute/
1992 Fall Meeting, Berkeley, CA, October 12–13, 1992,
and to be published in the Proceedings

Lewis Number Effects on Turbulent Premixed Flame Structure

P.J. Goix and I.G. Shepherd

September 1992

ENERGY & ENVIRONMENT
DIVISION

Prepared for the U.S. Department of Energy under Contract Number DE-AC03-76SF00098

LBL--32926

DE93 002571

Lewis Number Effects on Turbulent Premixed Flame Structure

P.J. Goix* and I.G. Shepherd†

*URA CNRS 230 CORIA BP 76134 Mt. St. Aignan FRANCE

†Energy and Environment Division
Lawrence Berkeley Laboratory
University of California
Berkeley, California, USA

September 1992

This work was supported by the Director, Office of Energy Research, Office of Basic Energy Sciences of the U.S. Department of Energy under Contract No. DE-AC03-76SF00098.

ABSTRACT

The influence of the Lewis number on turbulent flame front geometry is investigated in a premixed turbulent stagnation point flame. A laser tomography technique is used to obtain the flame shape, a fractal analysis of the multiscale flame edges is performed and the distribution of local flame front curvature is determined. Lean H_2/Air and C_3H_8/Air mixtures with similar laminar burning rates were investigated with Lewis numbers of 0.33 and 1.85 respectively. At the conditions studied the laminar H_2/Air mixture is unstable and a cellular structure is observed. Turbulence in the reactant stream is generated by a perforated plate and the turbulent length scale (3mm) and intensity (7%) at the nozzle exit are fixed. The equivalence ratio is set so that the laminar burning velocity is the same for all the cases. The results show clearly that the turbulent flame surface area is dependent on the Lewis number. For a Lewis number less than unity surface area production is observed. The shape of the flame front curvature distribution is not found to be very sensitive to the Lewis number. For the H_2/Air mixture the distribution is skewed toward the positive values indicating the presence of cusps while for the C_3H_8/Air mixture the distribution is more symmetrical. In both cases the average curvature is found to be zero, and if the local burning speed varies linearly with curvature, the local positive and negative burning velocity variations due to curvature will balance.

INTRODUCTION

Premixed combustion is involved in many practical systems such as propulsion, internal combustion engines and industrial burners. Laminar and turbulent combustion have been the object of intense experimental and theoretical research and the problem of laminar flame front dynamics has been addressed in detail by Law (1982) and Clavin (1985). It is clear from this work that Lewis number and hydrodynamic effects are significant factors in the dynamics of curved laminar flame fronts. In the wrinkled laminar flame regime, therefore, it is to be expected that Lewis number effects will modify the structure of premixed turbulent flame turbulent flames. The Lewis number, $Le = \alpha/\mathcal{D}$, is the ratio of the thermal diffusivity in the reactant mixture, α, and the mass diffusivity, $\mathcal{D}$, of the species deficient compared to the stoichiometric proportions and so it changes discontinuously from a lean to a rich mixture and from one fuel to another. Although significant simplifications in the modeling of turbulent combustion are obtained by assuming that the Lewis number is unity the range of applicability of this assumption has yet to be determined. Abdel-Gayed and Bradley (1989) have shown that the global quenching of premixed turbulent flames is sensitive to the Lewis number but its effects on turbulent flame structure are unclear. The object of this work is to focus on the influence of the Lewis number on the dynamics, structure and hence burning rate of low Reynolds number turbulent premixed flames. Specifically, the effect of laminar instabilities on the flame front surface area and modifications in flame front geometry in terms of the distribution of local flame front curvature will be investigated.

Flame surface area:

For high Damköhler number flames, where the chemical time is much shorter than the turbulence time, the increase in the mass burning rate can be correlated to an increase in flame front surface area caused by the turbulence in the approach flow. The turbulent burning velocity, S_T, is then:

$$S_T = S_L \frac{A_T}{A_L} \tag{1}$$

where A_T/A_L is the ratio between the turbulent and the laminar flame front surface areas and S_L is the laminar burning velocity. Gouldin (1987) has suggested that the turbulent flame front surface area may be obtained by fractal analysis.

If a multiscale object is a fractal it can be described by three parameters: the fractal dimension, D , and the inner and outer cutoffs, ε_i and ε_o respectively. In cases where the three fractal parameters can be evaluated there is a relationship between the area increase and ε_i, ε_o and D. The increase in length of a fractal line between these limits, obtained here from tomographic images, is given by :

$$\frac{L(\varepsilon_i)}{L(\varepsilon_o)} = \left(\frac{\varepsilon_i}{\varepsilon_o}\right)^{1-D_2} \qquad (2)$$

To obtain an estimate of the surface area increase it is often assumed that the flame surface is an isotropic fractal and that the fractal dimension of the flame surface, D_3, is related to that of the cross section line D_2, by $D_3 = D_2 + 1$. In the present case the outer cutoff is significantly larger, ~30mm, than the flame brush thickness, ~10mm, and this assumption is unlikely to be correct at the largest scales. The surface, however, is probably isotropic at scales smaller than the integral scale. As the flow field is identical for all the cases studied, the results can be compared directly and the isotropic estimate of the surface area will be adopted. The surface area increase, then, is given by:

$$\frac{A(\varepsilon_i)}{A(\varepsilon_o)} = \left(\frac{\varepsilon_i}{\varepsilon_o}\right)^{2-D_3} \qquad (3)$$

Combining (1) and (3) leads to :

$$S_T = S_L\left(\frac{\varepsilon_i}{\varepsilon_o}\right)^{2-D_3} \qquad (4)$$

Flame front curvature:

Markstein (1964) has proposed a relationship which includes the effects of the local flame front curvature and the strain rate of the reactant flow field on the flame front propagation velocity:

$$\left(\frac{S_n}{S_L} - 1\right) = \frac{\mathcal{L}}{S_L}\left(S_L h + \underline{n}\cdot\underline{\underline{\nabla u}}\cdot\underline{n}\right) \qquad (5)$$

where S_n is the normal burning velocity, S_L the unstrained laminar flame speed relative to the fresh mixture, $\mathcal{L}$ the Marstein length, h the local flame front curvature, $\underline{\underline{\nabla u}}$ the strain rate tensor in the flow field upstream of the flame front and $\underline{n}$ is the normal vector to the flame front directed toward the fresh mixture. The Markstein length depends on the physicochemical properties of the mixture and hence the Lewis number. An expression for the Markstein length which includes the temperature dependence of the diffusivities using high activation energy asymptotic analysis has been obtained by Clavin and Garcia (1983):

$$\mathcal{L}/d = \frac{1}{\gamma}\int_1^{\theta_b} \frac{r(\theta)}{\theta} d\theta + \frac{\beta(Le-1)}{2}\left(\frac{1-\gamma}{\gamma}\right)\int_1^{\theta_b} \ln\left(\frac{(\theta_b-1)}{(\theta-1)}\right)\frac{r(\theta)}{\theta} d\theta \quad (6)$$

where β is the Zeldovitch number, a reduced activation energy, and in this analysis $1/\beta << 1$. β is typically of order 10 for hydrocarbon flames, while for lean hydrogen flame it is of order 5. The heat release ratio, γ, is defined as: $\gamma=(\rho_u-\rho_b)/\rho_b$ where the subscript u represent unburned gas and b burned gas, d is the laminar flame front thickness, θ is the reduced temperature T/T_u and $r(\theta)$ is the ratio of the thermal diffusivities times the density at θ and in the reactant stream.

In summary then the Lewis number can affect the burning rate of premixed turbulent flames in two ways. First, the flame front instability may lead to the production of flame surface area and second, by changing the local reaction rate through the local flame front curvature. In this paper we will address experimentally these two issues by studying turbulent premixed flames over a range of Lewis numbers. A tomographic diagnostic technique which records flame front cross sections will be presented, a fractal analysis which is well adapted to a multiscale surface area analysis described and probability distributions of local flame front curvature obtained. The results will be interpreted in terms of the burning rate, and compared with results available in the literature.

EXPERIMENTAL DETAILS

The experiments presented in this paper have been performed on a stagnation point flame burner. A description of the flow field and flame structure results obtained by tomography have been published previously (1988,1990).

A fuel/air premixed flow is provided by a 50mm diameter jet, which is shielded by a concentric air stream at the same velocity of 100mm diameter. A stagnation plate is placed 100mm downstream of the burner exit and turbulence is generated by a perforated plate 50mm upstream of the burner exit and the turbulent length scale, l (3mm) and intensity (7%) at the nozzle exit are fixed. Cho et al. have found for this burner that these values do not change significantly until the flame zone is reached. The turbulent flame stabilizes at a distance from the stagnation plate determined by the mass consumption rate of the flame and the density ratio between the burnt and unburnt gases. An advantage of this configuration compared to the V-shaped or Bunsen flames is that the turbulent flame characteristics such as turbulent flame brush thickness and surface area are fixed in space. Goix et.al. (1988) have shown that the flame brush thickness and the flame surface area of a V-shaped flame increase monotonically downstream of the flame holder: differences of a factor of two or three being observed. Two mixtures have been chosen to investigate the effects of Lewis number on the structure of turbulent stagnation point flames: hydrogen/air and propane/air. The equivalent ratio in each case has been selected so that the mixtures have the same laminar burning velocity of S_L =30 cms^{-1}. The Lewis number and the turbulence and flow conditions are given in Table I.

High Speed Laser Tomography

A laser tomography technique based on Mie scattering which visualizes the location and shape of premixed flame front surfaces has been used extensively over the last ten years (Boyer, 1980; Goix et al., 1989; Chew et al., 1989; Zur Loye and Bracco, 1987). The scalar field of the premixed flames to be studied here consists essentially of burned and unburned states separated by a thin flame sheet and scalar properties, such as temperature or density, can be determined by measuring the intensity of light scattered from micron sized silicone oil droplets which evaporate at the flame sheet. A laser light sheet of 60mm width and 0.5mm thickness is produced by a copper vapor laser and two cylindrical lenses as shown in Fig (1). The copper vapor laser provides 5 mJ pulses of 20ns duration at adjustable repetition rates up to 10kHz at λ = 511nm. Silicon oil particles which evaporate at approximately 600K mark the leading edge of the flame sheet. A high speed Fastax camera was used to record the laser sheet and provide synchronization pulses at 3 kHz which trigger the laser. The film used was Kodak 4X reversal (400 ASA). The film frames are projected on a screen, digitized by a video camera and stored on a 512 x 512 I^2S matrix memory which has a dynamic range of 256 gray levels. The scaling factors in the X and Y directions are 0.16 mm per pixel and 0.12 mm per pixel respectively. A threshold corresponding to the maximum intensity gradient is determined from the gray level probability density function of each image and the flame front reaction zone edge corresponding to this threshold is extracted and stored for further statistical treatment. Since the gray level probability function is strongly bimodal around the area of interest (near the flame edges), the edge shapes were not sensitive to the threshold value selected for the edge detection. Digitization noise was removed from the edges by the method given in Shepherd et al. (1992). Representative flame edges for the three cases considered, an unstable hydrogen/air flame, and turbulent hydrogen/air and propane/air flames, are given in Fig. 2.

Many analysis methods are available to determine the fractal parameters from such data: e.g. the stepping caliper method, the box counting method and the circle method. The stepping caliper method has been used here because the flame boundaries are continuous and it has been shown to be the most sensitive by Shepherd et al. (1992). The flame length is determined by stepping along the flame boundary at a given scale ε_n. The flame length determined at that scale is then

$$L(\varepsilon_n) = N\varepsilon_n$$

Where N is the number of steps necessary to cover the whole flame length. The fractal dimension can be obtained by plotting in log-log space $L(\varepsilon_n)$ versus ε_n. The large scale cutoff, ε_o , and the small scale cutoff, ε_i , can also be obtained when a sharp change in slope is observed on both sides of the fractal region. The fractal parameters have been determined in a window of 40 *mm* about the stagnation line.

The curvature along the flame edge is obtained from a least mean square fit of a circle locally to the curve within the same window as in the fractal calculations. The sign of the curvature has been chosen to be positive when the flame front is concave toward the unburned gas.

RESULTS AND DISCUSSION

Unstable laminar hydrogen/air flame:

Laminar hydrogen /air flames are unstable at lean equivalence ratios due to Lewis number effects and cellular, self turbulizing flames are observed (Williams, 1985). In the present stagnation point configuration, however, the planar strain that the flame experiences will tend to stabilize the flame by damping perturbations of the flame front. As instabilities may play a significant role in the wrinkling process of a turbulent flame a preliminary investigation of an unstable laminar flame was conducted.

An equivalence ratio of $\phi \cong 0.3$ was found to be the threshold above which an unstable lean hydrogen/air laminar flame front is obtained. Fig 3. shows the growth of a cellular flame when the threshold is crossed; the time taken for the instability to develop was approximately 13 ms. The dark region in figure 3 is the hot product zone between the cold flow and the stagnation plate. The surface area of the flame is increased by the instabilities, fig. 2(a), and so the flame stabilizes at a higher approach flow axial velocity: 60 cm/sec compared to 30 cm/sec for the stable case. The velocities were determined by one dimensional LDV measurements along the stagnation line using as the seed silicon oil droplets which disappear at the cold boundary to give the mean flame propagation velocity at that point. The velocity gradient for all the cases is $dU/dx = 50\ s^{-1}$.

Fig 4(a) is a fractal plot of the chaotic, cellular hydrogen/air flame under laminar flow conditions obtained by averaging 30 independent flame edges. Using equation 3 and the fractal parameters in Table II, gives an increase in surface area above the stable, planar case of 1.19 which may be compared to the increase in flame propagation speed by a factor of 2. It should be noted that the measured inner cutoff is close to the laser sheet thickness of 0.5*mm* and the actual cutoff value may be smaller. Fig 4(b) shows the probability density function of flame front curvature deduced from the same data set. The average curvature was found to be very small, $\bar{h} \sim 0.0$, although a marked asymmetry, see Table III, can be observed toward large positive curvatures, which is characteristic of the presence of the flame cusps clearly visible in Fig 2(a).

Flame surface area:

The experimental conditions for the turbulent flames studied here are presented Table I and examples of the flame edges are shown in Figure 2 (b,c). For these cases the ratio u'/S_L is 1.2 and the Lewis number varies from Le = 0.3, for the lean H_2/air mixture, to Le = 1.85 for the lean propane/air mixture. Cho et al. (1986) found that the profile of the velocity rms was flat along the centerline of similar flames and so u'/S_L has been computed from the upstream turbulent conditions.

Since at high Damköhler numbers molecular effects control the local consumption rate, Lewis number effects (well described in the literature by Clavin (1985) and Williams (1985)) may play a significant role in the wrinkling process and resultant surface area of a turbulent premixed flame. Although fractal analyses of turbulent flames by Gouldin et al. (1988), Goix et al (1989), Takeno et al. (1990) and

Zur Loye and Bracco (1989) have shown that the increase in surface area is related to an increase in u'/S_L, the large scatter in these results indicates that a simple relationship does not exist between the fractal parameters and the turbulent flow field characteristics and that the wrinkling process of the surface is not a function solely of u' and S_L as proposed by North and Santavicca (1990).

Fig. 5(a,b) is a comparison between the fractal plots obtained from the flame front of the propane/air mixture and the hydrogen/air mixture. In this figure the plots, obtained by averaging 30 statistically independent edges, show that the edges are fractal, on average, over a range of scales of more than a decade. The ratio between the inner and the outer cutoffs is 13 for the propane mixture and 14 for the hydrogen mixture but the fractal dimension for the hydrogen mixture, D=2.25, is significantly higher than for the propane mixture, D=2.13. This difference represents, equations (3,4), a 40% difference in the area increase and hence burning rate and is also 65% higher than for the unstable laminar hydrogen/air flame. The increase in surface area per unit volume in the case of the hydrogen mixture, Le=0.33, is $A_T/A_L = 1.95$ compared to that of the propane mixture, Le=1.85, of $A_T/A_L = 1.41$. For these cases the turbulence conditions and the laminar burning velocities are the same and the ratio u'/S_L is identical for both cases. The cutoffs are not very sensitive to the Lewis number and move only slightly towards smaller scales for the hydrogen case, $(\varepsilon_i)_{H_2}/(\varepsilon_i)_{C_3H_8} = 0.86$ and $(\varepsilon_o)_{H_2}/(\varepsilon_o)_{C_3H_8} = 0.94$. The predominant effect of the Lewis number is to change the fractal dimension the cutoff sizes, Table II, being determined by the turbulence field. This effect may be explained by an amplification of the perturbations of the flame front produced between the cutoff scales by the velocity field. The density ratios of these two systems are different, however, and the greater expansion of the burned gases in the propane case may limit the area to volume ratio of the flame front and so contribute to reducing the fractal dimension. It is also of interest to note that the inner cutoff for the unstable laminar case is significantly smaller than in the turbulent case indicating again the importance of the perturbation field, the turbulence, in determining the significant wrinkle scales.

In Fig. 6 the surface area increase of turbulent stagnation point flames is plotted against the Lewis number as defined above, using the results presented here with results obtained by Shepherd et al (1990) for methane and ethylene mixtures at similar u'/S_L ratios. It is clear from this figure that the Lewis number is an important parameter in the wrinkling process of turbulent flames and in the case of lean mixtures, when the Lewis number is less than unity, surface area production is observed. Liu and Lenze (1989) in attempted a correlation between the turbulent burning rate and u'/S_L used mixtures of methane and hydrogen as the fuel. A significant difference between lean and the rich mixtures was observed in the burning rate increases and it was found that the burning rate ratio was always higher for the lean mixture at the same u'/S_L ratio even for high values of u'. It is probable that in modifying the fuel by adding hydrogen to the methane (which has a Lewis number of unity) Lewis number effects became important and so the lean mixtures behaved differently from the rich mixtures.

Flame front curvature:

The probability distributions for the local flame front curvature obtained from 30 flame images for the two turbulent flame cases (a) H_2/air and (b) C_3H_8/air mixture are compared in fig 7. The statistics of these distributions, calculated between $h = \pm 3mm^{-1}$, are given in Table III. Although only the pdf of the flame front curvature in the tomographic plane is measured, recent comparisons of such data with three dimensional direct numerical simulations indicate that a reasonable estimate of the pdf of the surface curvature can be obtained from the pdf of the planar curvature (Shepherd and Ashurst, 1992). As in the laminar case, the turbulent hydrogen/air pdfs are skewed towards the positive curvature while for the propane mixture the pdf is more Gaussian in shape indicating that some of the production of surface area in the hydrogen/air flame is occurring at large positive curvatures. The Markstein number, Ma=$\mathcal{L}$/d can be calculated using equation (6) for the lean propane/air mixture where the large Zeldovitch number assumption is valid (β=10) to give a value of 7.9, Table III. This assumption may not be acceptable for the hydrogen/air mixture where a value of β=5 has been used. Experimental determinations of the Markstein number have recently been performed by Searby and Quinard (1991) and Deshaies and Cambray (1990) over a range of conditions where propane, hydrogen, methane and ethylene/air mixtures were studied. They both found a linear relationship between the curvature and the difference in propagation and burning speed. The average curvature was found to be close to zero for all the cases studied and it may be concluded from equation 5 that the difference, on average, between the burning velocity and the local propagation speed will be depend on the straining field. In the case of the stagnation point flame configuration where the flame front is normal to the flow field close to the stagnation line the bulk strain term in equation (5) becomes: $\underline{n}\cdot\underline{\underline{\nabla u}}\cdot\underline{n} = (dU/dx)$ which was measured by LDV to be $50s^{-1}$. It should be noted that there will also be a fluctuating strain rate term due to the turbulence field which in the present case, if estimated by u'/l (~110), is larger than the mean strain. In this linear regime positive and negative curvature effects balance each other and the main impact of the Lewis number on the mass burning rate of the turbulent hydrogen flame is therefore to increase the flame front surface area. The linear dependence of the burning speed on flame stretch, however, could not be determined experimentally for the present lean hydrogen/air mixture and so the linear Markstein relationship is still an assumption for this condition. Furthermore, equation 5 has been derived from an asymptotic analysis for small curvatures and weak strain (Clavin, 1985) and the response of the flame at large flame stretch rates may well be non-linear.

CONCLUSION

In this paper the Lewis number effect on the shape of a turbulent premixed stagnation point flame front for study. C_3H_8/Air and H_2/Air lean mixtures were chosen to address this problem. The Lewis number of these mixtures is respectively Le=1.85 for the propane/air and Le=0.3 for the hydrogen/air mixture. The tomography technique has been has been used in order to record flame front edges. The flame front surfaces areas

have been analyzed with a fractal algorithm to estimate the flame surface area and probability density functions of local flame curvature deduced.

1) The laminar H_2/air stagnation point flame was found to be unstable above an equivalence ratio ϕ = 0.3. From the longitudinal velocity profiles the flame front propagation speed was deduced for the stable and self turbulizing flame. The ratio of these propagation speeds was equal to 2 which does not match the corresponding area increase of 1.19 obtained from the fractal analysis.

2) For the same turbulent flow conditions the turbulent flame front surface area was found to be sensitive to the Lewis number. This effect was predominantly in the fractal dimension which varied from 2.13 for the propane mixture to 2.25 to the hydrogen mixture corresponding to increases in surface area and hence burning rate of 1.41 and 1.95 respectively. The cutoffs are not very sensitive to the Lewis number and are probably determined by the turbulence field.

3) The flame front curvature distribution was not strongly dependent on the Lewis number. The distributions of the unstable and turbulent hydrogen/air mixtures were similar and found to be skewed toward positive curvatures (convex toward the burned gases) which can be attributed to the presence of cusps. For the lean propane mixture the curvature distribution is more symmetrical. In all cases, however, the average curvature was zero. If the laminar burning velocity is a linear function of the curvature these results indicate that positive and negative curvature effects on the local laminar burning speed balance and have no net effect on the average burning rate.

ACKNOWLEDGMENTS

The authors would like to express their appreciation to R.K. Cheng, and G.L. Hubbard from Lawrence Berkeley Laboratory for their assistance in the LDV setup, software for the flame front curvature determination and useful discussions.

REFERENCES

Boyer, L., "Laser Tomographic Method for Flame Front Movement Studies", *Combustion and Flame*, **39**, 3, (1980).

Cheng, R. K., Talbot, L., Robben, F., "Conditional Velocity Statistics in Premixed CH4-Air and C2H4-Air Turbulent Flames" *Twentieth Symposium (Int.) on Combustion/The Combustion Institute*, pp. 453-461, (1984).

Chew, T.C., Britter R.E., and Bray, K.N.C. "Laser Tomography of Turbulent Premixed Bunsen Flames", *Combustion and Flame*, **75**, (1989).

Cho, P., Law, C.K., Hertzberg, J.R. and Cheng, R.K. "Structure and Propagation of Turbulent Premixed Flames Stabilized in a Stagnation Flow" *21st Symposium Int'l on Combustion/The Combustion Institute*, pp. 1493-1499, (1986).

Clavin, P., "Dynamic Behavior of Premixed Flame Fronts in Laminar and Turbulent Flows", *Progress in Energy and Combustion Sciences*. **11**, No 1, (1985).

Deshaies, B., Cambray, P., " The velocity of a Premixed Flame as a Function of the Flame Stretch: An Experimental Study", *Combustion and Flame*, **82**, pp 361-375, (1990).

Goix, P.J., Paranthoen, P., and Trinite, M., "A Tomographic Study of Measurements in a V-Shaped H_2/Air Flame and a Lagrangian Interpretation of the Turbulent Flame Brush Evolution", accepted, *Combustion and Flame*, (1989).

Goix, P.J., Shepherd, I.G., Trinite, M., "A Fractal Study of a Premixed V-Shaped H2/Air Flame", *Combustion Science and Technology*, **63**. pp. 275-286 (1989).

Gouldin, F.C., "An Application of Fractals to Modeling Premixed Turbulent Flames", *Combustion and Flame*, **68**, no. 3, June (1987).

Gouldin, F.C., Hilton, S.M., and Lamb, T., "Experimental Evaluation of the Fractal Geometry of Flamelets", published in the *22nd Symposium Int'l on Combustion/The Combustion Institute*, Seattle (1988).

Gouldin, F. C., Bray, K., N., C., Chen, J.Y., "Chemical Closure Model for Fractal Flamelets", *Combustion and Flame*, **77**, pp 241,259 (1989).

Liu, Y., Lenze, B., " Investigation on the Combustion-Turbulence Interaction in Premixed Flames Using Tomography and Laser Doppler Velocimetry", *22nd Symposium International on Combustion*, Seattle (1988)

Mandelbrot, B.B., "Fractal Geometry of Nature", "W.H. Freeman and Company", New York, (1983).

Markstein, G.H., "Nonsteady Flame Propagation", Pergamon Press, (1964).

North, G. L., Santavicca, D. A., "The Fractal Nature of Premixed Turbulent Flames", *Combustion Sciences and Technology*, **72**, pp 215-232, (1990).

Searby, G., Quinard, J., "Direct and Indirect Measurements of Markstein Number of Premixed Flame", *Combustion and Flame*, **92**, pp 298-311, (1990)

Shepherd, I. G., Cheng, R. K.and Talbot, L., Experimental Criteria for the Determination of Fractal Parameters of Premixed Turbulent Flames", *Experiments in Fluids*, (to be published), (1992).

Shepherd, I.G., Cheng, R. K., Goix, P. J., " The Spatial Structure of Premixed Turbulent Stagnation Point Flames", *23rd Int. Symposium on Combustion*, Orleans (1990).

Shepherd, I.G. and Ashurst, Wm.T., "The Flame Front Geometry of Premixed Turbulent Flames", to be presented at *24th Int. Symposium on Combustion,* Sydney, 1992.

Sreenivasan, K.R. and Meneveau, C., "The Fractal Facets of Turbulence", *Journal of Fluid Mechanics*,**17**, pp.357-386, (1986).

Sreenivasan, K.R., Prasad R.R, Fractal dimension of scalar interfaces in turbulent jets, *Polish Acad. Sci.*, **14**, 1-14, (1988).

Takeno, T., Murayama, M., Tanida, Y. "Fractal analysis of turbulent premixed flame surface", *Experiment in Fluids*, **10**, pp. 61-70, (1990).

Williams, F.A., "Combustion Theory" 2nd Edition. The Benjamin-Cummings Publishing Company, Inc. (1985).

Zur Loye, A. O., Bracco, F. V., "Two-Dimensional Visualization of Premixed-Charge Flame Structure in an IC engine", *International Congress and Exposition*, Detroit Michigan February 23-27, 1987.

CAPTIONS

Fig. 1 Schematic of high speed laser tomography experiment.

Fig. 2 Flame front edges obtained from tomography: (a) unstable laminar hydrogen/air flame (b) turbulent hydrogen/air flame (c) turbulent propane /air flame

Fig. 3 Time series of 6 tomography snapshots taken at 3 kHz of an unstable premixed laminar hydrogen/air stagnation flame. $\phi = 0.3$

Fig. 4(a) Fractal plot of a laminar cellular H_2/air flame.

Fig. 4(b) Probability density function of curvature of the laminar cellular flame.

Fig. 5 Fractal plots of turbulent flame front edges. (a) H_2/Air mixture (b) C_3H_8/Air mixture.

Fig. 6 Turbulent to laminar flame front surface area ratio versus the Lewis number for turbulent premixed stagnation point flames.

Fig. 7 Probability density function of curvature of the turbulent stagnation point flame. (a) H_2/air mixture (b) C_3H_8/air mixture

TABLE I:

Mixture and Flow field Conditions

	C_3H_8	H_2
ϕ	0.75	0.30
T_b/T_u	6.60	4.00
Le	1.85	0.33
S_L *m/s*	0.30	0.30
u' *m/s*	0.35	0.35

TABLE II

Fractal Results

	H_2 (unstable)	H_2 (turbulent)	C_3H_8
D	2.06	2.25	2.13
ε_i *mm*	0.60	1.32	1.62
ε_o *mm*	9.3	19.8	21.1
A_T/A_I	1.2	1.95	1.41

TABLE III

Flame Front Curvature

	H_2 (unstable)	H_2 (turbulent)	C_3H_8
h mm^{-1}	-0.0002	-0.031	-0.006
h' mm^{-1}	0.61	0.87	0.51
skewness	0.84	0.83	0.76
kurtosis	3.76	3.98	5.7
Ma	1.7	1.7	7.9

HIGH-SPEED TOMOGRAPHY

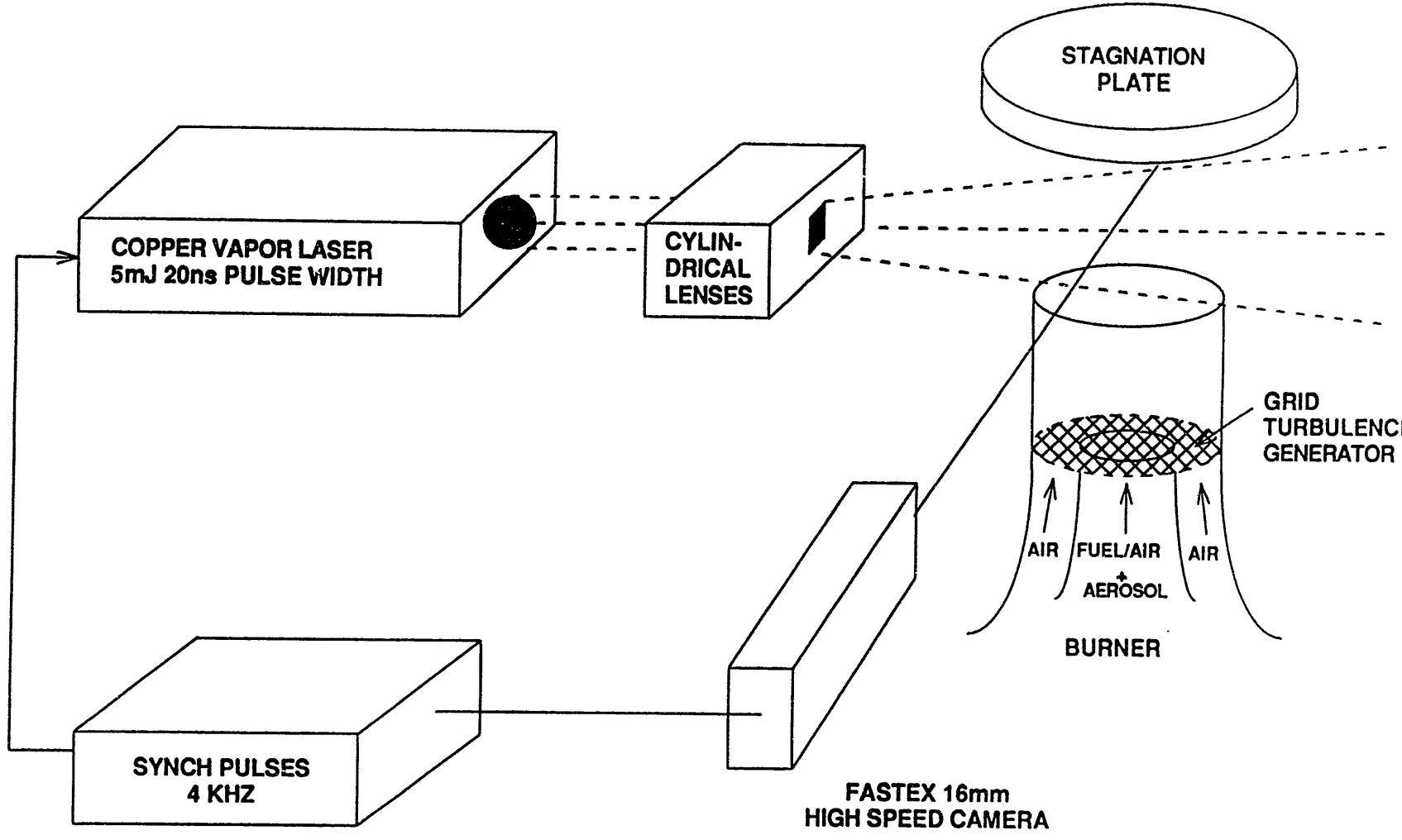

FIGURE 1

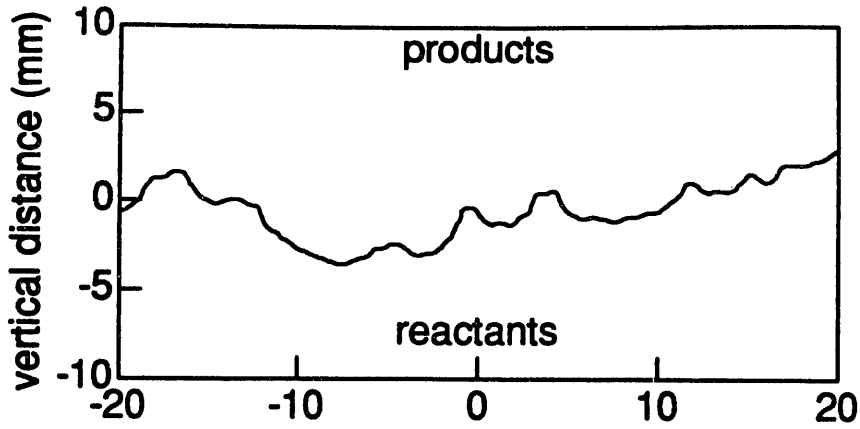

(a) Laminar hydrogen/air flame (unstable)

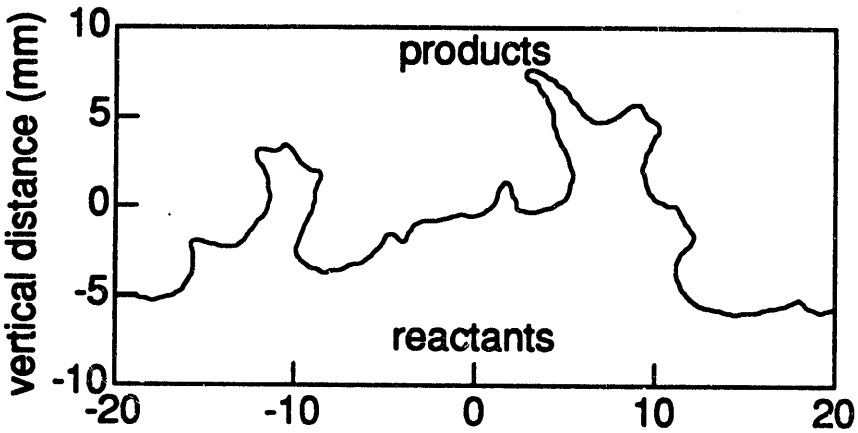

(b) Turbulent hydrogen/air flame

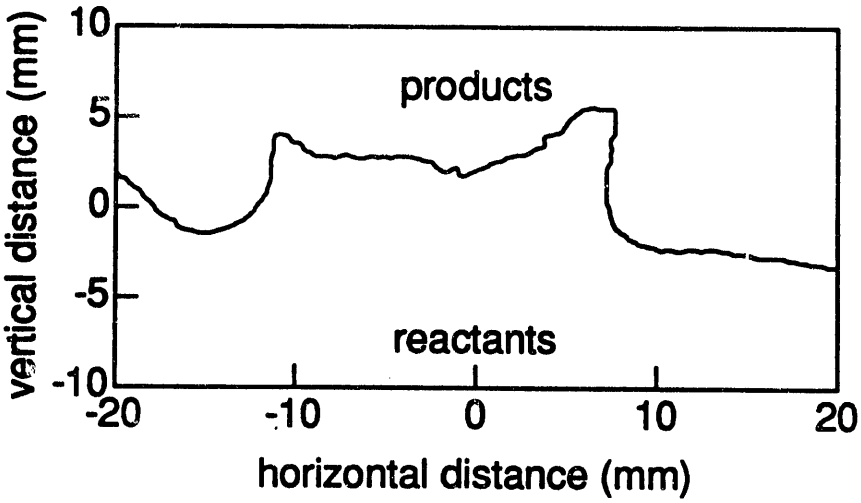

(c) Turbulent propane/air flame

FIGURE 2

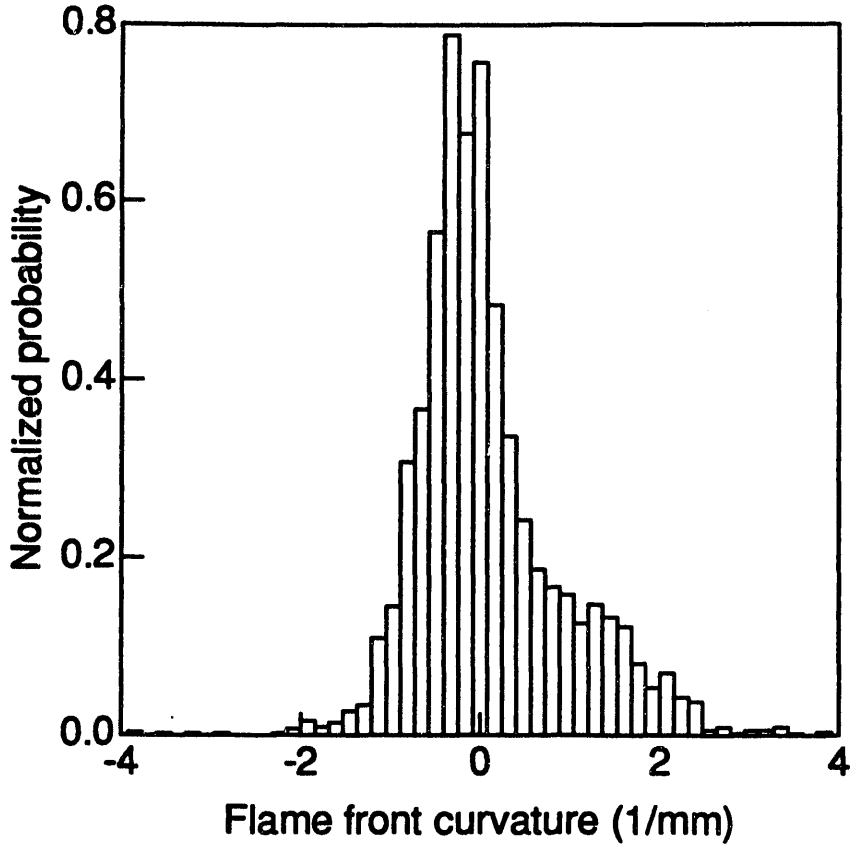

Fig 4b. Hydrogen/air flame (unstable), curvature

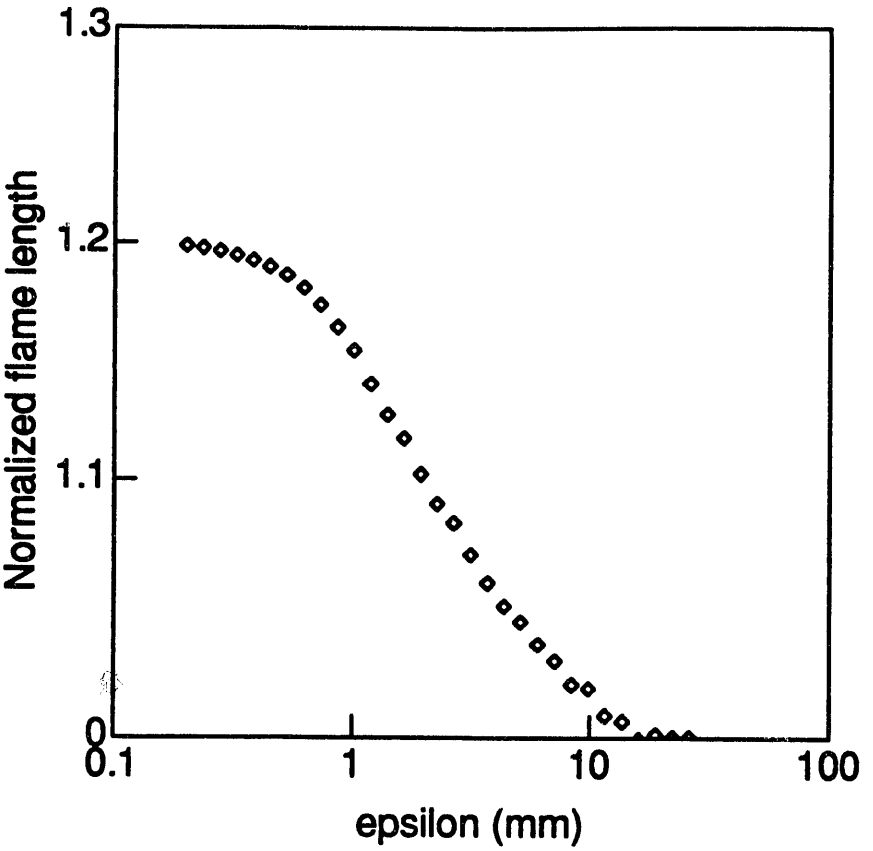

Fig 4a. Hydrogen/air flame (unstable), fractal plot

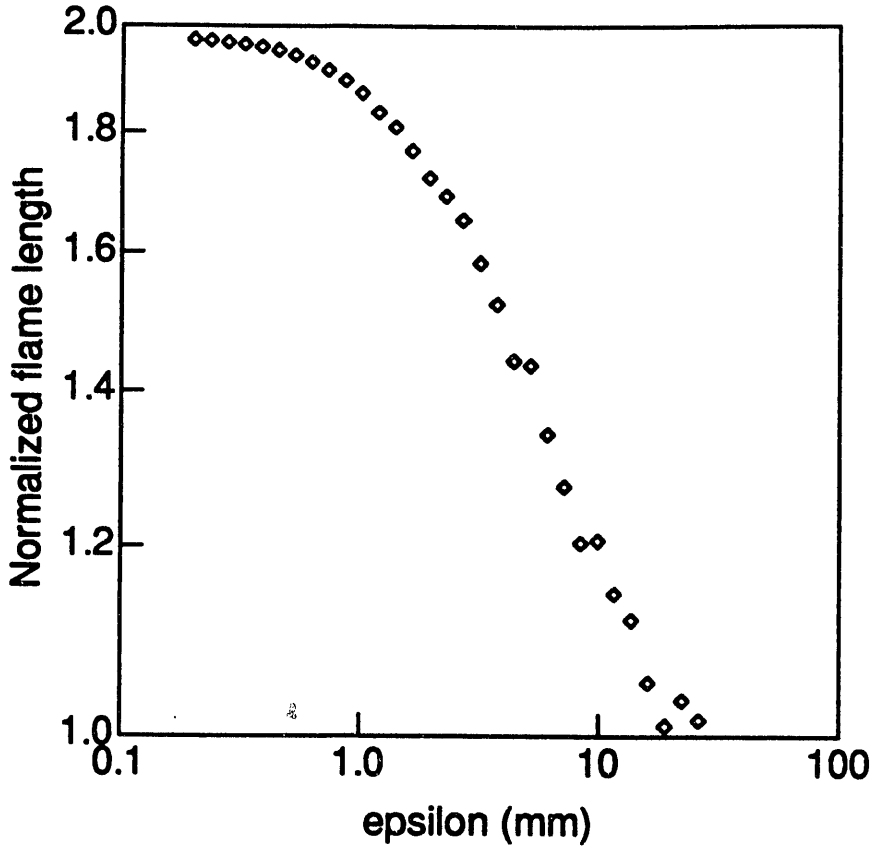

Fig 5a. Hydrogen/air flame (turbulent), fractal plot

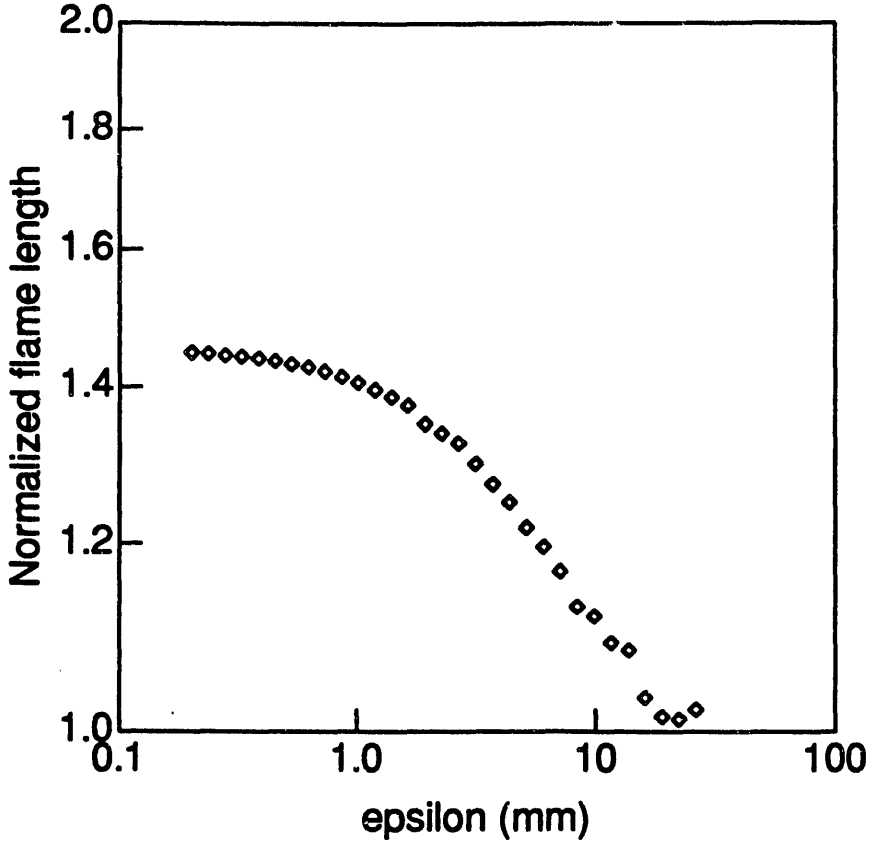

Fig 5b. Propane/air flame (unstable), fractal plot

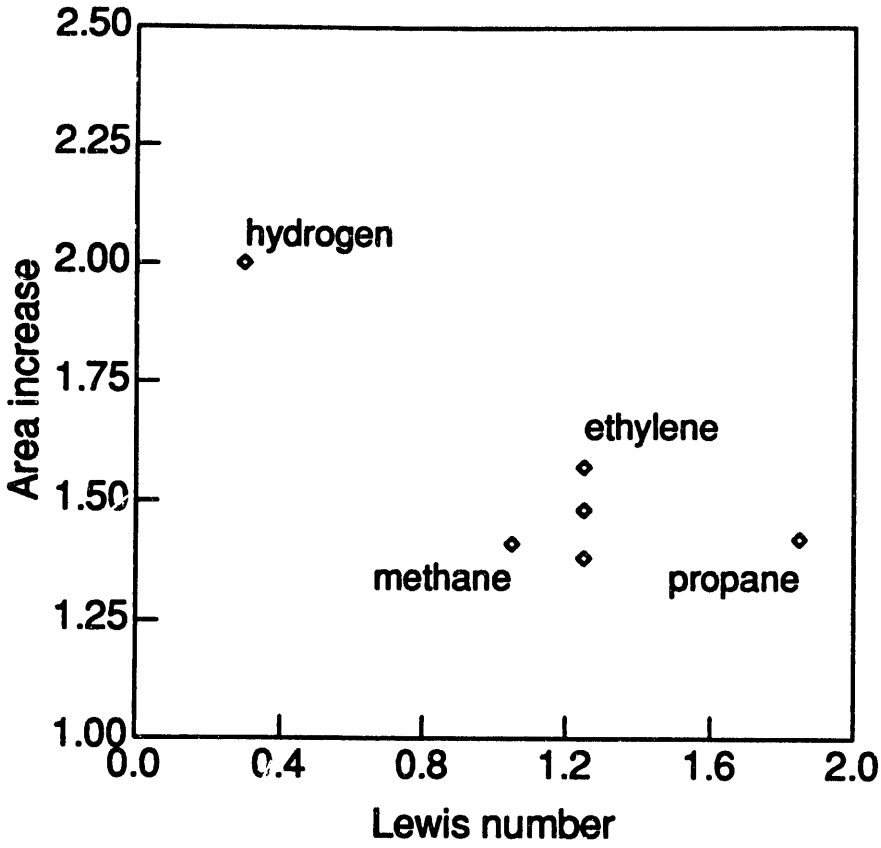
2.50
2.25
2.00
1.75
1.50
1.25
1.00
Area increase
hydrogen
ethylene
methane
propane
0.0
0.4
0.8
1.2
1.6
2.0
Lewis number

FIGURE 6

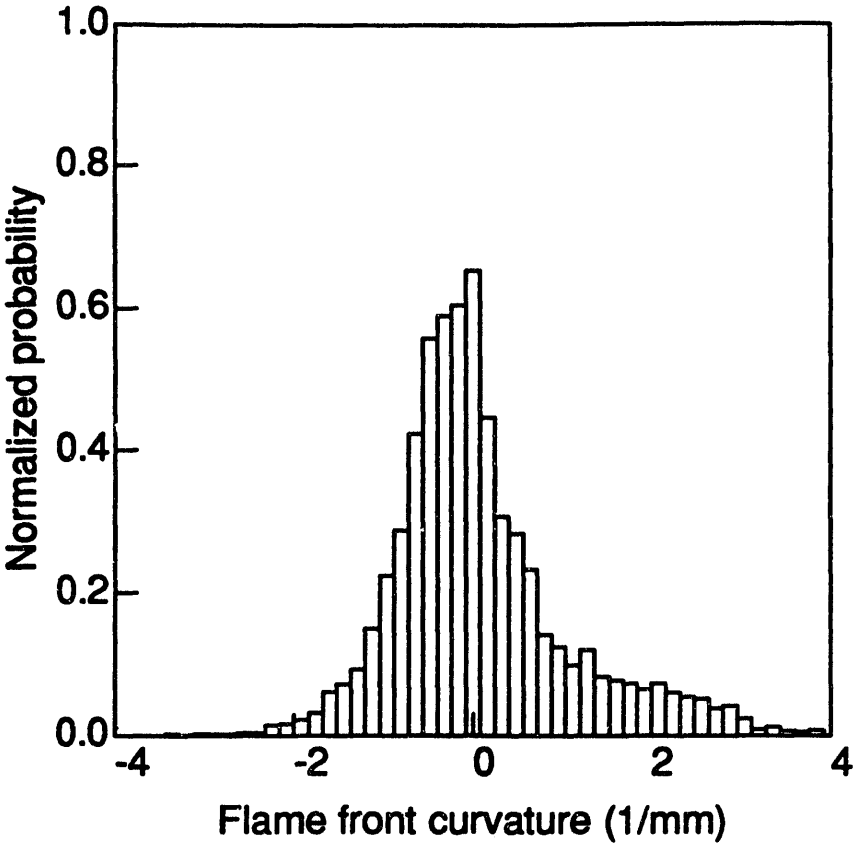

Fig 7a. Hydrogen/air flame (turbulent), curvature

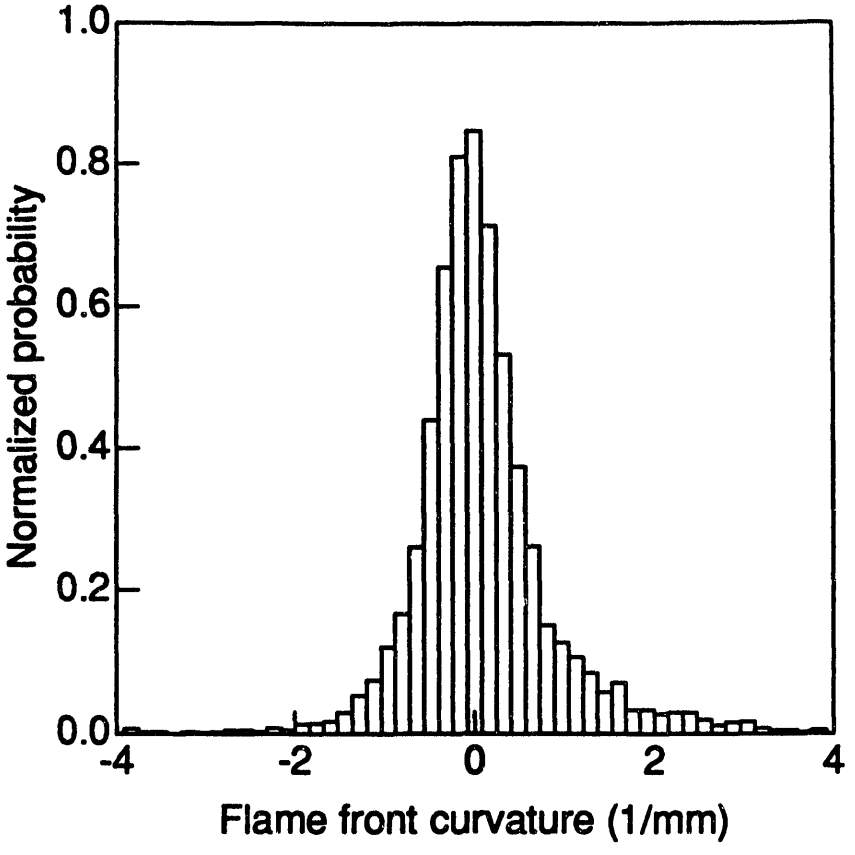

Fig 7b. Propane/air flame (turbulent), curvature

DATE
FILMED
01/22/93